Force and Motion Generation of Molecular Motors: A Generic Description

Frank Jülicher

Institut Curie, Physicochimie Curie, Section de Recherche, 26 rue d'Ulm, 75248 Paris Cedex 05, France

Abstract. We discuss a general model to study force and motion generation of motor molecules which move along linear filaments that are polar and periodic. A 4-state model motivated by the reaction cycle can be simplified by keeping only two states. The remaining two-state model can be used to describe many physical aspects of biological motor proteins. We review generic properties of this model and discuss collective effects which can occur in many-motor systems. These collective effects include dynamical instabilities of the steady states and the possibility to generate oscillations.

1 Introduction

An essential and striking features of living cells is their ability to generate motion and forces. Important examples are cell motility, the contraction of muscles but also active phenomena within cells that allow for material transport and the motion of organelles, for example during cell division and mitose. All of these movements and forces are generated on the molecular level by protein molecules that are driven by chemical reactions in a far from equilibrium situation. Important examples are motor proteins, enzymes which are specialized to work as motors. In eucariotic cells, several families of motor proteins exist which interact with the cytoskeleton, a complex three-dimensional elastic network of long rod-like filaments inside the cell which is essential for the mechanical stability and integrity of the cell [2].

A motor protein of the cytoskeleton interacts specifically with a certain type of filament along which it is able to move in presence of Adenosinetriphosphate (ATP) which is a chemical fuel. The filaments serve as guides or tracks for the motion. Two types of filaments play this role: microtubules and actin filaments. Both are formed by a polymerization process from identical monomers (actin and tubulin monomers, respectively), leading to a regular and periodic structure. An important feature is their polarity: The filaments are asymmetric with respect to their two ends. This follows from the monomers which themselves are asymmetric, leading to a polar filament structure with two different ends which are denoted "plus end" and "minus end". This polar symmetry is essential for motor operation as it defines the direction of motion. Motor proteins are classified into several families: myosins, kinesins and dyneins. Myosins move always along actin filaments

and towards the plus end. Kinesins and dyneins move along microtubules, kinesins move towards the plus end and dyneins towards the minus end, see Fig. 1.
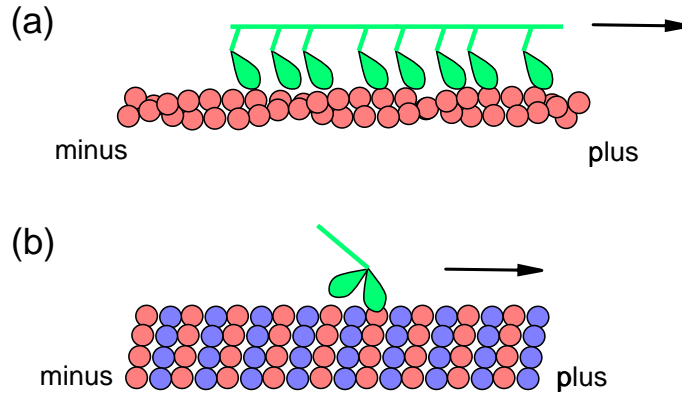

Fig. 1. Schematic representation of molecular motors and track filaments. (a) myosin interacting with actin filaments. (b) kinesin moving along a microtubule. Both types of filaments are polar and periodic, their two different ends are denoted "plus" and "minus".

Myosins are prominent for their role in the contraction of muscles [24, 26]. In this case, many myosin molecules form a linear structure, a myosin filament, which interacts with actin filaments arranged in parallel. The action of myosin motors then induces the relative sliding of the two types of filaments. In muscle cells, a very large number of filaments is organized in a regular way which on a macroscopic scale leads to the muscular contraction. Myosins also occur within normal cells where they are important for cell motility and the organization of actin. Kinesins occur in large numbers in neurons, where they play a key role in transport of vesicles along the axon towards the synapse. Both types of motors have two identical heads of a size of about 10-20nm which are the elementary force-generating elements as well as a tail which is used to attach the motor to another structure [31].

The chemical fuel plays an important role in this process. The hydrolysis reaction $ATP \rightarrow ADP + P$ of ATP to Adenosinediphosphate (ADP) and Phosphate (P) is used as a source of chemical energy. The motor protein M (or more precisely, the head domain containing the ATP binding site) undergoes a chemical cycle: it binds ATP and hydrolizes the bound ATP. Subsequently it releases the products ADP and P. We denote the different chemical states by M, M-ATP, M-ADP-P, and M-ADP, respectively. After completion of the cycle (M+ATP $\rightarrow$ M-ATP $\rightarrow$ M-ADP-P$\rightarrow$ M-ADP+P $\rightarrow$ M+ADP+P) the motor is unchanged. However, during this process it has
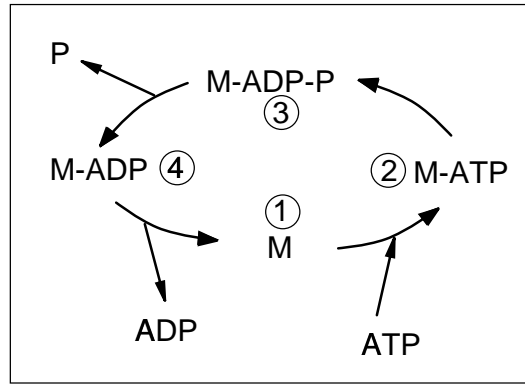
Fig. 2. Chemical cycle of a motor molecule M. After completion of the cycle on molecule ATP is hydrolyzed to ADP and phosphate (P).

undergone conformational changes and it has hydrolyzed one ATP molecule, see Fig. 2. The different conformations which occur during the chemical cycle in general have different geometries and properties and can in particular have different interaction characteristics with respect to the filament [25]. As a result, the motor protein undergoes chemistry-driven changes between strongly and more weakly bound states ("attachments" and "detachments"). This coupling between chemistry and binding permits the creation of motion along a polar filament [22, 48].

The force and motion generation of individual or groups of motor proteins can be studied experimentally by a variety of techniques. In so-called motility assays, motors are attached to a substrate [32, 21, 27, 53]. Filaments in solution bind to the motors and in presence of ATP start moving along the surface. In these experiments typically several or many motors interact with a single filament.

In order to observe the forces generated by an individual motor, the processivity of the motor becomes important. Myosin is not processive. During the chemical cycle it detaches from the filament during a significant period of time. During this time it can easily diffuse away from the filament if it is not held in place. Forces generated by single myosin molecules have been observed by different techniques, see Fig. 3 (a) and (b). Micron sized bead have been coated with low density of motors and optical traps have been used to bring a filament in contact with the bead and possibly only a single motor [15]. Forces on the filament are then measured by observing the displacement in the trap. Another possibility is to fix the actin and to manipulate the bead with an optical trap. Such experiments reveal that the motor induces stochastic displacements of the order of $5 - 10$nm which last for several milliseconds and peak forces of the order of 1pN [15, 27].
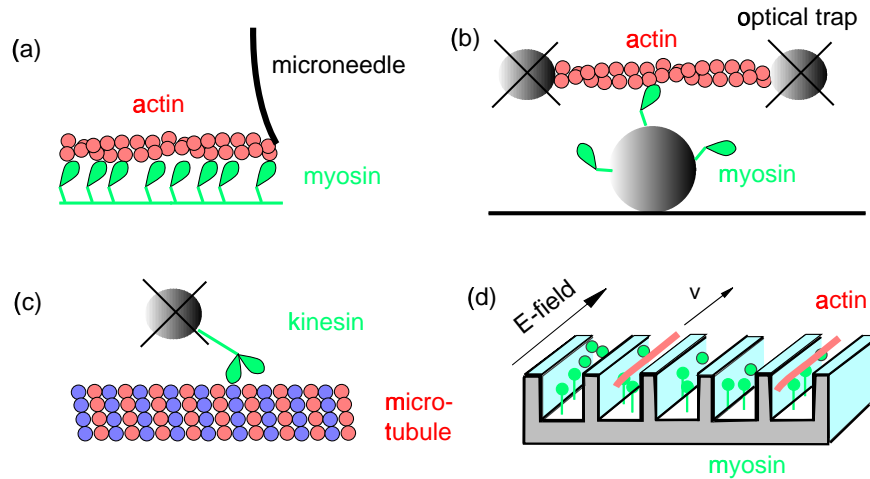
Fig. 3. Examples for micro-manipulation experiments. (a) Forces induced my myosin on actin can be measured by the deflection of a micro-needle [27]. (b) Force measurement using optical traps [15]. (c) Forces generated by a single kinesin molecule observed by displacements of a bead in an optical trap [50]. (d) Forces induced by an electric field E in a motility assay using linear grooves to orient the filaments [45].

Kinesin, is a processive motor [5]. A single kinesin moves along micro-tubules for a distance of the order of micrometers before losing the filament. Motion of single kinesin molecules can therefore be observed directly, either by attaching a small bead to the motor and observing the displacement of the bead or by directly marking the molecule with a fluorescent dye. Optical traps have been used to study the velocity of motion as a function of an applied load [50]. It has been shown, that kinesin moves in a step-wise fashion with characteristic steps of 8nm size [49]. This step size coincides with the period of kinesin binding sites along microtubules which demonstrates that the ATP-driven reaction cycle induces steps between periodically spaced binding sites. The characteristic time-scales for kinesin motion are milliseconds and forces up to 5pN are generated [50, 23].

It is widely believed that the processivity of Kinesin becomes possible because of the fact that each molecule consists of *two* head domains which both hydrolize ATP and undergo the chemical cycle in a coordinated way [5]. They very rarely detach from the filament at the same time allowing the motor to keep attached while displacing. Single heads do have the capability to generate forces and motion but current experiments indicate that they are not processive. Myosin molecules also often have two heads. However, even with both heads they do not become processive since every myosin head has

a tendency under normal operating conditions to be unbound during about 90% of its chemical cycle.

From the point of view of a general classification of the physical mechanisms which can lead to motion generation, motor proteins fall in a class of systems characterized by the fact that they operate on *molecular scales* and generate motion along a one-dimensional polar and periodic structure (sometimes called ratchet [14]) by a non-equilibrium *rectification process* [6, 33, 1, 36, 3, 11, 4]. For a system on a molecular scale, fluctuations play an important role for its function and properties. These fluctuations can be both of thermal origin or they can arise due to the stochasticity of individual molecule chemical reactions. Therefore, a theoretical description requires the use of concepts of non-equilibrium statistical physics. Biological motor proteins are the most prominent examples for these systems. However, there is a growing number of artificially designed "molecular motors" [46, 13, 19, 20], suggesting that the physics of these systems is relevant for micro-and nano-technological devices.

In the subsequent sections, we describe a simple modelization of the generic aspects of these systems, using biological motor proteins as a guide. In section 2 we introduce the basic concepts of such a modelization. Properties of single motor motion which follow from this description are described in Sect. 3. In section 4, we discuss the consequences of many motor systems and demonstrate that new phenomena such as dynamical instabilities follow naturally from these models. Finally, we present in section 5 a discussion and an outlook.

2   Simplified models

In order to keep the description simple and to focus on generic properties, we do not aim to capture microscopic structural details of biological motor proteins. We use a simplified picture taking into account the periodicity and polarity of the linear track and the fact that during the chemical cycle conformational changes occur [30].

The main assumption required for this simplification is a separation of time-scales [22, 30]. Even though a macromolecule like a protein is characterized by a large number of microscopic degrees of freedom, most of them relax on time scales shorter than the typical relevant time scales for the chemical cycle. These degrees of freedom are therefore to a good approximation thermally equilibrated. Only a few slow degrees of freedom have to be described by dynamical equations. These relevant degrees of freedom are collective modes of the system. Examples are chemical reaction coordinates but also the overall position variable of the motor with respect to the filament. The latter is important in order to describe the coupling between chemistry and motion.

2.1   Energy landscapes and chemical transition rates

Following Ref. [22], we assume for simplicity that the chemistry of s single head can be described by a number m of discrete states or conformations $i = 1..m$. Many biochemical models focus on the four states M, M-ATP, M-ADP-P, M-ADP but other reaction intermediates could also be included [35, 22]. Changes between these states are fast compared to the typical time between transitions and the mechanical action or motion of the motor. Therefore we use a chemical kinetics description for changes between states.

If we consider a motor in conformation i, we can define a potential or interaction energy profile along the filament. Suppose that one small region of the motor, e.g. in the tail, is used to transmit forces or to attach a cargo. We imagine this point to be held at a position x along the filament. We can now define $W_i(x)$ to be the energy of the motor, including possibly bound ATP, ADP or P, and including the energy of the filament as the motor is held at position x. This total energy is in fact an effective free energy obtained by averaging over all rapidly relaxing microscopic degrees of freedom but keeping the enzyme in its chemical state. The conformation of the system motor-filament is then fully characterized by the pair $\{i, x\}$ of internal state and position with respect to the filament. Note, that the potentials reflect the symmetry properties of the filament. If the filament is polar and a periodic array of identical monomers, the potentials are periodic with period l, $W_i(x) = W_i(x + l)$ and asymmetric, $W_i(x) \neq W_i(-x)$.

In order to describe the dynamics of the system $\{i, x\}(t)$, we use a stochastic overdamped dynamics at constant temperature T within a given state i

$$\eta_i \frac{d}{dt} x = -\partial_x W_i(x) + \zeta_i(t) \quad . \tag{1}$$

Here η_i is a protein friction and $\zeta(t)$ is a Gaussian white noise in state i with $< \zeta_i(t)\zeta_j(0) >= 2\eta_i\delta(t)$. The chemical reactions between states $\{i, x\}$ and $\{j, x\}$

$$\{i, x\} \quad \overset{\omega_{ij}(x)}{\underset{\omega_{ji}(x)}{\rightleftharpoons}} \quad \{j, x\} \tag{2}$$

occur with Poisson statistics with reaction rates $\omega_{ij}(x)$. Since the position variable x is also a conformational degree of freedom (the motor in general changes its shape while displacing), transition rates are in general x-dependent. Note, that for simplicity in Eq. (2) we have assumed that transitions between states happen instantaneously and without displacement. Furthermore, we have used the fact that thermal relaxation is very fast compared to the chemical cycle and all rapid degrees of freedom are equilibrated at constant temperature T. In fact, the typical relaxation time of temperature gradients which have developed on a length scale l can be estimated as

$\tau = Cl^2/\kappa$, where C is the specific heat of the material per volume and κ the thermal conductivity. Using typical values for water and length scales of the order of 10nm we find $\tau \simeq 10^{-6} - 10^{-8}$s, which is fast compared to typical cycle times of several ms. This argument shows that the motor operates isothermally, i.e. temperature gradients are not created and cannot be used to generate motion as e.g. in the case of Feynman's ratchet [14].

It is now convenient to use a Fokker-Planck description [44] and to introduce distribution functions $P_i(x,t)$ for the probability to find within an ensemble of identical systems the motor at time t at position x in state i. These distributions then obey the equations

$$\partial_t P_i + \partial_x J_i = \sum_{j \neq i} (\omega_{ji}(x) P_i(x) - \omega_{ij}(x) P_j(x)) \tag{3}$$

$$J_i = \eta_i^{-1}(-k_B T \partial_x P_i - P_i \partial_x W_i + P_i f_{\text{ext}}) \quad . \tag{4}$$

The total density and total current

$$P(x,t) = \sum_{i=1}^{m} P_i \tag{5}$$

$$J(x,t) = \sum_{i=1}^{m} J_i \tag{6}$$

obey the conservation law $\partial_t P + \partial_x J = 0$. The average velocity in the steady state with stationary and periodic distribution function $P_i(x) = P_i(x+l)$, $\partial_t P_i = 0$ is given by

$$v = \int_0^l J dx / \int_0^l P dx \tag{7}$$

In order to characterize the chemical rates, we first introduce the chemical potentials of the fuel and hydrolysis products in bulk solution. We denote μ_{ATP}, μ_{ADP} and μ_P the free energy per ATP, ADP or P molecule, respectively. As an illustrative example, we first consider the four chemical states M ($i = 1$), M-ATP ($i = 2$), M-ADP-P ($i = 3$) and M-ADP ($i = 4$), often encountered for biological motor proteins. A general reaction kinetics for all eight reaction rates which is consistent with the ATP hydrolysis reaction can be written by using four different kinetic coefficients:

$$
\begin{array}{ll}
\omega_{12} = \alpha_1 \exp[(W_1 + \mu_{ATP})/k_B T] & \omega_{21} = \alpha_1 \exp[W_2/k_B T] \\
\omega_{23} = \alpha_2 \exp[W_2/k_B T] & \omega_{32} = \alpha_2 \exp[W_3/k_B T] \\
\omega_{34} = \alpha_3 \exp[W_3/k_B T] & \omega_{43} = \alpha_3 \exp[(W_4 + \mu_P)/k_B T] \\
\omega_{41} = \alpha_4 \exp[(W_4 + \mu_P)/k_B T] & \omega_{14} = \alpha_4 \exp[(W_1 + \mu_{ADP} + \mu_P)/k_B T]
\end{array}
\tag{8}
$$

Here, we have used the condition of detailed balance of the rates. The functions $\alpha_i(x)$ characterize the possible reaction scenarios. Note, that since transitions are fast and therefore occur for fixed x, the chemical rates do not

depend on the external force f_{ext} or local stresses. Force-dependent are only displacements described by equation (1). The present modelization differs in this respect from models which use discrete transitions also to describe displacements. In this case chemical rates are strain dependent [22, 34, 12]. From a physical point of view, all models are of course equivalent.

2.2   Two-state models

It is useful to further simplify the generic description introduced above. The m-state model allows in principle to describe many details of the chemical cycle and the various conformations of the motor. However, it contains a large number of free parameters which are unknown. It is therefore useful to further simplify the model. In fact, in order to describe physical aspects of motion generation and force generation, it is sufficient to keep only two different states [1, 42, 39].
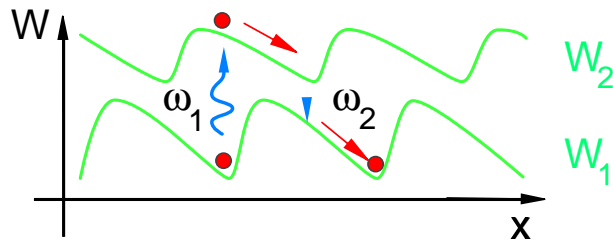

Fig. 4. Two state model defined by two polar and periodic potentials W_1 and W_2 as well as periodic transition rates ω_1 and ω_2. Pumping between the two states induces average motion.

We rewrite the Fokker-Planck equations (4) for two states $i = 1, 2$:

$$\partial_t P_1 + \partial_x J_1 = -\omega_1(x)P_1 + \omega_2(x)P_2$$
$$\partial_t P_2 + \partial_x J_2 = \omega_1(x)P_1 - \omega_2(x)P_2 \quad , \tag{9}$$

where we have introduced $\omega_1 = \omega_{12}$ and $\omega_2 = \omega_{21}$ and the currents are the same as introduced in Eq. (4). This system is sketched in Fig. 4 for an example of shifted periodic and asymmetric potentials.

This two-state model is still very flexible and allows to describe situations which capture many of the physical aspects of biological protein motors. Fig. 5 shows choice of potentials W_1 and W_2 adapted to the commonly accepted picture of myosin function [48]: a myosin head detaches from the actin filament after binding ATP. In the unbound state ATP is hydrolyzed (M-ATP$\rightarrow$ M-ADP-P). The head (M-ADP-P) is now again able to bind actin. As it encounters a binding site along the filament, it reattaches under phosphate
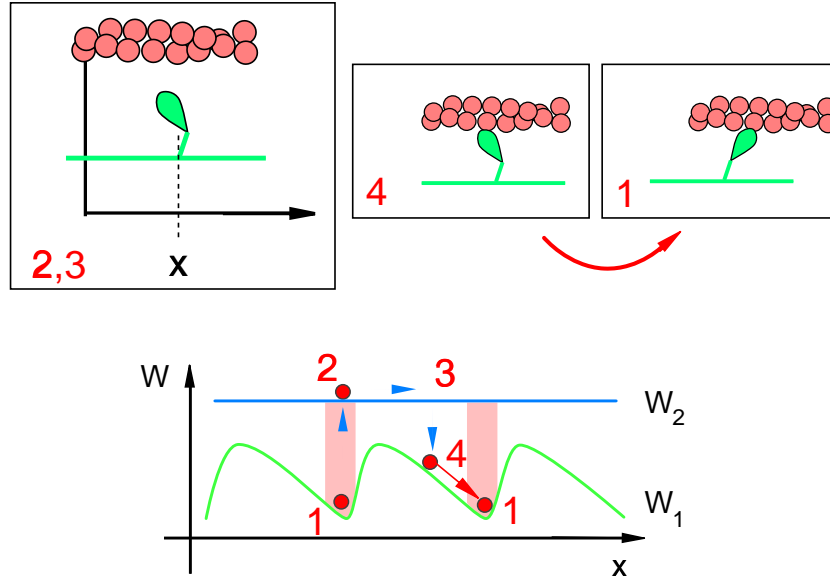
Fig. 5. Two state model representing a situation motivated by the functioning of myosin. (1) Binding an ATP molecule, myosin detaches from actin (2). After hydrolysis (3), it rebinds and generates a force (4) and a displacement. In a two state model, two potentials W_1 and W_2 characterize attached and detached states with the tail at position x. The shaded areas are "active sites" where ATP-driven transitions occur.

release. After reattachment, a force-generating step occurs and ADP is released, which completes the chemical cycle. As illustrated in Fig. 5 this process can be captured by two different potentials, W_1 and W_2 representing the unbound state (a flat potential) and the bound state (a potential with periodic structure) respectively. After the force-generating step (power-stroke), the x variable has reached a potential minimum. Here, the system can be actively excited to the unbound state under ATP binding. As it reattaches to the filament, the slope of the potential reflects the mechanical force generated at this point. A displacement is generated as the system slides downhill along the energy profile to reach the potential minimum. Note, that microscopically this displacement could correspond either to a tilt of the head domain as sketched in the figure or to other more complex processes. The microscopic structure associated with this displacement is not characterized by this description.

In a two-state picture, the chemical reaction cycle as described by the kinetic equations (8) has to be divided into two substeps. One possibility is to introduce the forward and backward rates α_1 and α_2 for the combined process of ATP-binding and hydrolysis

$$M + ATP \overset{\alpha_1}{\underset{\alpha_2}{\rightleftharpoons}} M\text{-ADP-P} \quad , \tag{10}$$
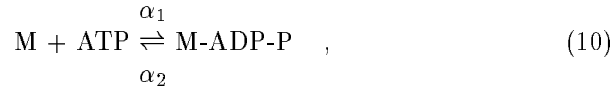
and the rates β_1 and β_2 which describe the process of product release and binding:

$$M + ADP + P \overset{\beta_1}{\underset{\beta_2}{\rightleftharpoons}} M\text{-ADP-P} \quad . \tag{11}$$
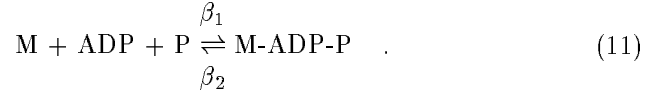
The complete chemical cycle is now the subsequent transitions α_1 and β_2. As long as α_2 and β_1 are nonzero, there is a nonvanishing probability for an inversion of the cycle (i.e. ATP generation) by following the steps α_2 and β_1. We define W_1 to be the energy of a free motor together with the product molecules (M + ADP + P) and W_2 to be the energy of the complex M-ADP-P. Detailed balance of the chemical reactions then implies

$$\frac{\alpha_1}{\alpha_2} = e^{(W_1 - W_2 + \Delta\mu)/k_B T} \tag{12}$$

$$\frac{\beta_1}{\beta_2} = e^{(W_1 - W_2)/k_B T} \quad , \tag{13}$$

where we have introduced the chemical driving force

$$\Delta\mu \equiv \mu_{ATP} - \mu_{ADP} - \mu_P \quad . \tag{14}$$

The transition rates of the two-state model are the superpositions $\omega_i = \alpha_i + \beta_i$. Introducing two unknown functions $\alpha(x)$ and $\beta(x)$ which describe conformation dependent energy barriers, we can therefore write

$$\omega_1(x) = \alpha(x)e^{(W_1 + \Delta\mu)/k_B T} + \beta(x)e^{W_1/k_B T}$$
$$\omega_2(x) = [\alpha(x) + \beta(x)]e^{W_2/k_B T} \quad . \tag{15}$$

Note, that other choices to divide the reaction cycle in two relevant substeps leads to the same result, but redefines the arbitrary functions α and β and shifts the potential W_2 by a constant value.

The functions $\alpha(x)$ and $\beta(x)$ define the coupling of the chemical reaction to conformation. Very important is the concept of localized or conformation-dependent transitions where the functions are peaked within a narrow x-interval but negligible outside this interval. An example is the ATP-binding step which in Fig. 5 is restricted to occur within an "active region" of conformation space corresponding to the potential minimum while the conformations at the beginning of a force-generating power stroke are not supposed to bind ATP. As we will describe in the subsequent sections, the localization of transitions via the functions α and β plays an important role in defining the mechanical properties of these systems.

Similar to the case of myosin, the two state model can also be adapted to more complex situations such as kinesin motion. For kinesin in most situations the action of two heads both of which contain an ATP binding site
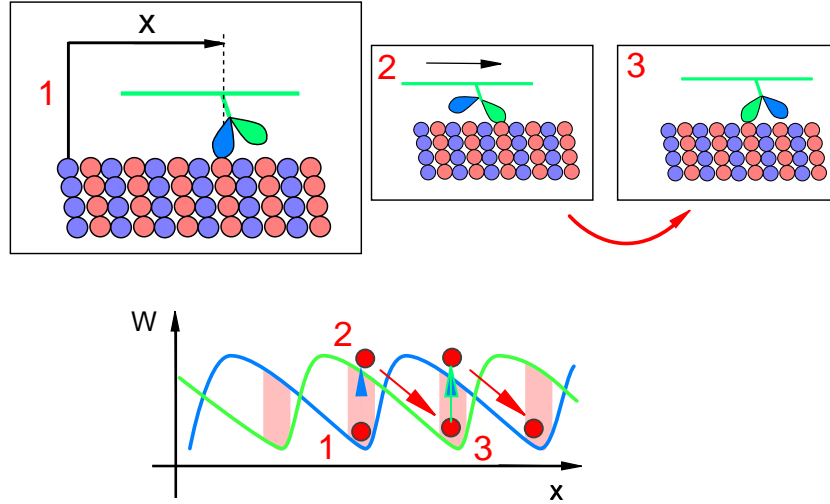
Fig. 6. Hand over hand motion suggested for kinesin. At any time, one head is bound and the second head moves towards the next binding site. This situation can be represented by describing both heads by identical but shifted energy landscapes $W_1(x)$ and $W_2(x)$.

is important. Therefore, a general description would require eight internal states and a complex reaction scenario. A possible simplification arises from the fact that there is growing evidence for a coordinated binding and unbinding of the two heads in a hand-over-hand fashion as shown schematically in Fig. 6 [5]. Such a coupling would reduce the number of relevant degrees of freedom of the protein [40]. In a two-state model, this feature can be captured in a simplified way by associating each state with one of the heads being bound to the filament. Denoting the motor with head 1 or head 2 bound to the filament by M_1 and M_2, respectively, we define the energies of these situations $\bar{W}_1$ and $\bar{W}_2$. Because the two heads forming a kinesin motor are identical, the energy landscapes of both states are two identical potential profiles which are shifted with respect to each other by one monomer period $l/2$ on the filament: $\bar{W}_1(x) = \bar{W}_1(x + l)$; $\bar{W}_2(x) = \bar{W}_1(x + l/2)$, see Fig. 6. However, the characteristic step-size of an individual head l in this picture corresponds to two monomer sizes. Therefore, the potentials $\bar{W}_i$ are l-periodic, while the total system is invariant under $x \to x + l/2$ if at the same time the two states are exchanged. Therefore the transition rates also obey $\omega_1(x) = \omega_1(x + l)$ and $\omega_2(x) = \omega_1(x + l/2)$. Again, the idea of active regions and localized transitions is important. Assuming that all transitions occur at conformations which correspond to the potential minimum, we obtain a system which operates in an almost deterministic way where the chemical cycle

is closely correlated to a particular displacement. In the case of non-localized transitions, the chemical cycle is related to motion in a more irregular way.

A useful representation of the transition rates in the hand-over-hand picture is to assume that a full ATP hydrolysis cycle changes M_1 to M_2:

$$M_1 + ATP \rightleftharpoons M_2 + ADP + P \quad . \qquad (16)$$
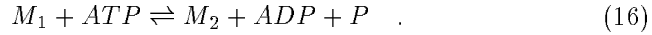
Because of the symmetry between the two heads, the reaction $M_2 + ATP \rightleftharpoons M_1 + ADP + P$ occurs with the same rates. This leads to the total transition rates

$$
\begin{aligned}
\omega_1(x) &= e^{\bar{W}_1(x)/k_BT}[\bar{\alpha}(x)e^{\Delta\mu/k_BT} + \bar{\alpha}(x+l/2)] \\
\omega_2(x) &= e^{\bar{W}_2(x)/k_BT}[\bar{\alpha}(x) \qquad\quad + \bar{\alpha}(x+l/2)e^{\Delta\mu/k_BT}\}]
\end{aligned}
\qquad (17)
$$

The unknown function $\bar{\alpha}(x) = \bar{\alpha}(x + l/2)$ is l-periodic. Note, that the choice given in Eq. (17) is a special case of Eq. (15) if we identity $\alpha(x) = \bar{\alpha}(x)e^{\Delta\mu/2k_BT}$, $\beta(x) = \bar{\alpha}(x+l)e^{\Delta\mu/2k_BT}$ and $W_i = \bar{W}_i - \Delta\mu/2$. This example demonstrates that Eq. (15) is a general choice which can describe all types of couplings of a ATP hydrolysis to a two state model.

We have now defined a two-state model which can describe a system undergoing an ATP hydrolysis cycle and moving along a periodic structure. As discussed above, this model is sufficiently flexible to be adapted to situations which resemble the widely accepted pictures of myosin and kinesin functioning.

3   Single motors

We will now discuss general properties of the two-state model for a single motor introduced above [42, 7, 8]. Two generalized forces act on the system leading to an out-of equilibrium situation. These are the chemical "force" $\Delta\mu$ introduced in Eq. (14) and the mechanical force f_{ext}. If both generalized forces are kept constant, the system eventually attains a steady state with $\partial_t P_i = 0$. The steady state distribution functions satisfy two coupled differential equations of second order

$$
\begin{aligned}
k_BT\partial_x^2 P_1 + (\partial_x P_1)(\partial_x W_1 - f_{\text{ext}}) - P_1\partial_x^2 W_1 &= \eta(\omega_1 P_1 - \omega_2 P_2) \\
k_BT\partial_x^2 P_2 + (\partial_x P_2)(\partial_x W_2 - f_{\text{ext}}) - P_2\partial_x^2 W_2 &= -\eta(\omega_1 P_1 - \omega_2 P_2)
\end{aligned}
\quad , (18)
$$

where we have for simplicity assumes that the friction η is the same for both states. This set of equations together with periodic boundary conditions $P_i(x) = P_i(x + l)$ defines the steady state distributions. They can be calculated in special cases analytically, but in general numerical integration techniques are used. For each pair $(\Delta\mu, f_{\text{ext}})$, there is a uniquely defined average velocity

$$v = \frac{1}{\eta} \int_0^l dx [P_1(f_{\text{ext}} - \partial_x W_1) + P_2(f_{\text{ext}} - \partial_x W_2)] \quad , \qquad (19)$$

where the P_i satisfy the normalization condition

$$\int_0^l dx[P_1 + P_2] = 1 \quad .$$
(20)

Similarly, we can introduce the ATP hydrolysis rate r which denotes the number of chemical cycles performed per unit time [30]. Using the rates introduced in Eqns. (10) and (11),

$$r = \int_0^l dx[\alpha_1 P_1 - \alpha_2 P_2] = \int_0^l dx[\beta_2 P_2 - \beta_1 P_1] \quad .$$
(21)

If $\Delta\mu = 0$, the transition rates defined by Eq. (15) satisfy

$$\omega_1/\omega_2 = e^{-\Delta W/k_B T} \quad ,$$
(22)

where

$$\Delta W(x) = W_2(x) - W_1(x) \quad .$$
(23)

This condition of detailed balance for the total transition rates indicates that transitions are just thermal fluctuations and that the system is not driven chemically. If the external force also vanishes, the steady state is a thermal equilibrium with $P_i = Ne^{-W_i(x)/k_B T}$ for which $v = 0$ and $r = 0$. For $\Delta\mu > 0$, the system is chemically driven. If no external force is applied spontaneous motion with $v \neq 0$ can occur, however only if the system is polar. For a symmetric system with $W_i(x) = W_i(-x)$ and $\omega_i(x) = \omega_i(-x)$ the steady state distributions are also symmetric $P_i(x) = P_i(-x)$. Since $\partial_x W_i$ is antisymmetric in this case, $v = 0$ by symmetry according to Eq. (19). On the other hand, r is in general nonzero in this case (the functions α_i are symmetric). For spontaneous motion to occur two requirements have to be fulfilled: detailed balance of the transition has to be broken, which corresponds to $\Delta\mu \neq 0$ and the system must have polar symmetry. In the case of motor proteins the polar filaments play this role.

In the presence of an external force f_{ext}, the system can perform mechanical work, i.e. it operates as a motor. The work performed per unit time against the external force is

$$\mathcal{W} = -f_{ext}v$$
(24)

while the chemical energy consumed per unit time is given by

$$Q = r\Delta\mu \quad .$$
(25)

We can therefore define the efficiency of energy transduction

$$\eta = -\frac{f_{ext}v}{r\Delta\mu}$$
(26)

This quantity is useful for forces applied opposite to the direction of motion where $0 \leq \eta \leq 1$. Note, that this definition relies on the fact that a bulk

solution exists which plays the role of a thermodynamic reservoir and allows to define the chemical potentials of fuel and products. In practical situations the reservoirs may be small and not in local equilibrium. In such a case the efficiency would be more difficult to define.

For a discussion of physical aspects of motion, it is useful to write

$$\omega_1(x) = \omega_2(x)(\Omega(x) + e^{-\Delta W/k_B T}) \quad , \tag{27}$$

where

$$\Omega(x) = e^{-\Delta W/k_B T}(e^{\Delta\mu/k_B T} - 1)\alpha/(\alpha + \beta) \tag{28}$$

measures locally the rate of transitions violating detailed balance. Using the dependence of the chemical potential on particle concentration, $\mu_i = \mu_i^0 + k_B T \ln C_i$, we observe that

$$\Omega \sim \left(\frac{C_{ATP}}{C_{ADP} C_P} - k^0\right) \quad , \tag{29}$$

where $k^0 = e^{(\mu_{ATP}^0 - \mu_{ADP}^0 - \mu_P^0)/k_B T}$ is the equilibrium constant of the hydrolysis reaction. Ω therefore is a direct measure of the distance from chemical equilibrium. From Eqns. (28) and (29) we find

$$\Omega \sim \begin{cases} \Delta\mu & \text{for} \quad \Delta\mu/k_B T \ll 1 \\ C_{ATP}/C_{ADP} C_P & \text{for} \quad \Delta\mu/k_B T \gg 1 \end{cases} \tag{30}$$

For our discussion of the two-state model it is useful to characterize the system by the functions ω_2 and Ω instead of α and β which allows us to discuss motion generation without the need to introduce chemistry. This choice is more general and can be used also for cases where transitions between states are triggered by other processes than chemistry such as in artificially constructed systems [46, 13, 19].

The properties of this two-state models have been discussed in Refs. [1, 7, 8, 30]. Calculating the average velocity v as a function of the externally applied force f_{ext} typically leads to a behavior which is well approximated by a linear dependence

$$v \simeq v_0(1 - (f_{\text{ext}}/f_s)) \tag{31}$$

for many different choices of the potential shapes and the transition rates. Here v_0 is the spontaneous velocity at zero force $f_{\text{ext}} = 0$ and f_s the stalling force, i.e. the force for which the system stops moving. Deviations from this linear behavior mainly occur for forces larger than the stalling force $|f_{\text{ext}}| > |f_s|$ or for forces parallel to its natural direction of motion $f_{\text{ext}}/f_s < 0$.

The observed force-velocity curves for kinesin motors show an almost linear behavior which can be characterized by v_0 and f_s defined in (31). While $f_s \simeq 5pN$ does not depend much on experimental conditions, the no-load velocity v_0 depends on ATP concentration and attached viscous loads and is of the order of $1\mu/s$ or smaller [51, 23].

The orders of magnitude observed for kinesin can be reproduced by the two-state model. Using a choice of potentials as shown in Fig. 6 with transition localized at the potential minimum, the stall force is approximatively given by the potential slope. Using a potential amplitude of $U \simeq 10 k_B T$ which is set by the available chemical energy of $\Delta\mu \simeq 10 - 15 k_B T$ and a period of $l \simeq 8nm$ of microtubules, this force is $f_s \simeq U/l = 5$pN consistent with the observed value. The spontaneous velocity of the two-state model can be estimated by $v_0 \simeq l/(t_c + t_s)$, where t_c is the time of the chemical steps and $t_s \simeq l^2\eta/U$ is the sliding time in the potential. Therefore, the observation of v_0 does not fix both the chemical rate and the value of η corresponding to protein friction. One estimate for the unknown friction η is to assume a hydrodynamic friction with a viscosity η_{vis} a factor $10^2 - 10^3$ larger than the one of water, suggesting $\eta \sim \eta_{\text{vis}}l \sim (1-10)10^{-8}$kg/s. This increased viscosity takes into account that the dissipation of proteins should be better represented by the viscous behavior of polymer solutions. A different approach is to assume that for large ATP concentration $t_c \simeq \omega_2^{-1}\Omega^{-1}$ is negligeable and the friction η determines the sliding velocity $v_0 \sim U/l\eta$. Estimating the maximal velocity $v_{\text{max}} \sim 10^{-5}$m/s, we find $\eta \sim 10^{-7}$ which can be seen as an upper bound since chemical steps which also contribute to friction are neglected.

A key parameter characterizing the conditions of operation of the two-state model is the the dimensionless value $U/\xi l^2 \Omega\omega_2$ which compares the typical chemical transition time with sliding times in the potential slope. With the arguments given above we estimate $U/\xi l^2 \Omega\omega_2 \simeq 0.1 - 1$, where we have used $\Omega\omega_2 \simeq 10^3$s^{-1} which is a typical transition rate [18]. However, different values are also consistent with the observed force-velocity relation as the spontaneous velocity v_0 is determined by the longest of the two time scales mentioned above. Additional information such as velocity fluctuations would be required to determine this value from experimental observations and to fix the orders of magnitude of all parameters of the model. Aside from this problem, the two state model produces typical velocities and forces as observed for kinesin with the observed force velocity relation showing that it is consistent with the observations. Other types of models which use different representations of states and transitions can also be used to consistently describe the force-velocity relation of kinesin [40, 12, 10].

4   Collective Effects: Dynamic Instabilities

In many biological situations, motor molecules and filaments do not operate as isolated enzymes but many motors are integrated in larger structures. Typical examples are actin/myosin in muscles and dyneins/microtubules in flagella and cilia. Furthermore, the presence on motor molecules in the cytoskeleton leads to complex physical properties of these systems on large scales [37].
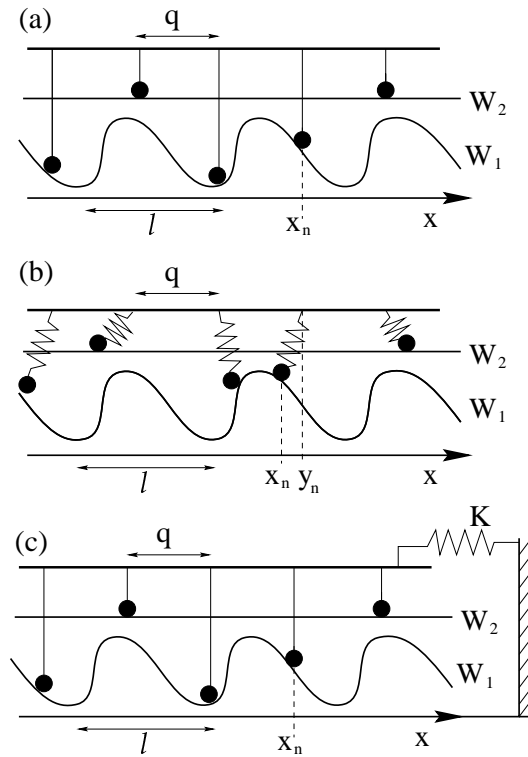
Fig. 7. Many motor system as rigidly coupled two-state models. (a) rigid coupling (b) elastic coupling to rigid backbone (c) elastic coupling to environment.

The most prominent many-motor system is actin/myosin in muscles. In this case, myosin molecules are attached together by their tails to form a linear filament. Myosin filaments and actin filaments are arranged in parallel in a highly organized fashion. In the presence of ATP they slide with respect to each other which macroscopically leads to muscle contraction. Experimental in vitro "motility assays" can be used to study myosin function in an artificial environment. In these systems, myosin molecules are attached to a solid substrate using specific antibodies. Actin filaments in solution adsorb to the myosin coated surface and start to move in presence of ATP as a result of the action of myosin motors [21, 48, 53, 45].

Another example are cilia and flagella which are elastic linear extensions of many cells which generate a beating motion used to propel the cell within a solvent or to move the solvent. A flagellum typically contains 9 pairs of microtubules, each pair coupled by a large number of dynein motors and other proteins which serve as structural elements. The motors create forces

that lead to the bending and motion of the flagella. Interestingly, these motors are used to generate oscillating motion [2].

These systems demonstrate that the behavior of systems containing motors can on larger scales have new and different types of behaviors than the one observed for individual motor molecules. As a first approach to discuss the behavior of many motor systems, we generalize the two-state model to describe a large number of coupled motors [28, 29, 30]. A simple modelization of such a situation is sketched in Fig. 7 (a). Many motors which all are described by a two-state model are attached along a linear backbone with constant spacing s. Assuming that the spacing between motors is fixed implies that the backbone is rigid. Within this assumption all motors have the same velocity. In practical cases, elastic properties of the filaments and of a backbone coupling the motors can become important. For example in the case of muscles, the passive elastic behavior of proteins such as titin can play the role of elastically coupling motor-filament systems to their environment [2]. Similarly, in flagella, bending elasticity of the filaments is essential to allow for the generation of beating motion. Fig. 7 (b) and (c) sketches two simple ways to incorporate the effects of material elasticity in the modelization.

4.1   Mean field limit

Motors coupled via a rigid backbone allow to illustrate the appearance of collective effects. For a system of N elements with two states, moving along a periodic structure, we can introduce the distribution function $p(x, \sigma_1, ..., \sigma_N)$ for finding the particles $i = 1..N$ in states $\sigma_i = 1, 2$ with particle i at position $x + si$ along a linear coordinate. This system thus becomes an effective 2^N-state system described by 2^N equations

$$\partial_t p(x, \sigma_1, .., \sigma_N) + \partial_x j(x, \sigma_1, .., \sigma_N) = -\sum_{i=1}^{N} \omega_{\sigma_i}(x + is)p(x, \sigma_1, .., \sigma_N)$$
$$+ \sum_{i=1}^{N} \omega_{\bar{\sigma}_i}(x + is)p(x, \sigma_1, .., \bar{\sigma}_i, .., \sigma_N) \quad (32)$$

Here, $\omega_\sigma(x) = \omega_\sigma(x + l)$ are the individual transition rates defined in the previous sections and the bar denotes the opposite state, i.e, $\bar{1} = 2, \bar{2} = 1$. The currents are given by

$$j(x, \sigma_1, .., \sigma_N) = \frac{1}{\eta N} \left[-k_B T \partial_x p - N p \partial_x w(x, \sigma_1, .., \sigma_N) - N p f_{\text{ext}} \right] \quad , \quad (33)$$

with the potential

$$w(x, \sigma_1, .., \sigma_N) = \frac{1}{N} \sum_{i=1}^{N} W_{\sigma_i}(x + is) \quad , \quad (34)$$

defined as a sum of individual particle potentials. Here, ηN denotes the total friction which is assumed to scale linearly with N and f_{ext} is the externally applied force per motor.

In order to reduce the number of equations and to obtain a tractable description, we introduce the average density of particles found at position $\xi = x \bmod l$, $0 \leq \xi \leq l$ relative to the potential period:

$$P_k(\xi) = < \rho_k(\xi) > \quad , \tag{35}$$

where

$$\rho_k(\xi) = \frac{1}{N} \sum_{i=1}^{N} \delta_{k,\sigma_i} \delta(x + is - \xi) \quad . \tag{36}$$

Here, we have introduced the notation

$$< a > = \lim_{m \to \infty} \frac{1}{2m} \int_{-ml}^{ml} dx \sum_{\sigma_1 .. \sigma_N} a(x, \sigma_1, .., \sigma_N) p(x, \sigma_1, .., \sigma_N) \quad , \tag{37}$$

for averages over the distribution p which we assume to be periodic, $p(x, \sigma_1, .., \sigma_N) = p(x+l, \sigma_1, .., \sigma_N)$ normalized over one period l, $< 1 > = 1$. The densities $P_k(\xi)$ satisfy the normalization condition Eq. (20) and behave like a single particle two-state model

$$\partial_t P_1 + \partial_\xi J_1 = -\omega_1 P_1 + \omega_2 P_2$$
$$\partial_t P_2 + \partial_\xi J_2 = \omega_1 P_1 - \omega_2 P_2 \quad , \tag{38}$$

however with the currents

$$J_k(\xi) = -\frac{k_B T}{N\eta} \partial_\xi P_k - < \rho_k(\xi) v > \quad , \tag{39}$$

where $v(x, \sigma_1, .., \sigma_N) = -[\partial_x w(x, \sigma_1, .., \sigma_N) + f_{\text{ext}}]/\eta$. From now on, we consider a large number N of motors and we assume that the period of motors is incommensurate with the potential period, s/l irrational. In this case, the total particle distribution function $P_1 + P_2 = < \sum_{i=1}^{N} \delta(\xi - x - is)/N >$ becomes homogeneous:

$$P_1(\xi) + P_2(\xi) = \frac{1}{l} + O(1/N) \quad , \tag{40}$$

and we can approximate $< \rho_k(\xi) v > = < \rho_k(\xi) > < v > + O(1/N)$. Ignoring terms of order $1/N$ including the diffusive term in Eq. (39) the currents simplify to

$$J_k(\xi) = v P_k(\xi) \quad , \tag{41}$$

where

$$v = < v > = \frac{1}{\eta} \left[-\int_0^l d\xi (P_1 \partial_\xi W_1 + P_2 \partial_\xi W_2) + f_{\text{ext}} \right] \quad . \tag{42}$$

We have found a simple mean-field theory which is very useful to explore the properties of a many-motor system. Ignoring all corrections in $1/N$, we finally obtain

$$\partial_t P_1 + v\partial_\xi P_1 = -(\omega_1 + \omega_2)P_1 + \frac{\omega_2}{l} \tag{43}$$

$$v = \frac{1}{\eta}\left[\int_0^l d\xi\, P_1 \partial_\xi \Delta W + f_{\text{ext}}\right] \tag{44}$$

which describes the time-evolution of $P_1(\xi) = 1/l - P_2(\xi)$.

4.2 Steady states

First, we look at the properties of steady state solutions with $\partial_t P_1 = 0$ and constant velocity which obey [28]

$$v\partial_\xi P_1 = -(\omega_1 + \omega_2)P_1 + \omega_2/l \quad , \tag{45}$$

where v is a parameter. Eq. (45) can be solved analytically for simple choices of the transition rates. A more general approach is a power expansion of the steady state in the velocity

$$P_1(\xi) = \sum_{n=0}^{\infty} P_1^{(n)}(\xi)v^n \quad , \tag{46}$$

where the $P_1^{(n)}$ satisfy the recursion relation $P_1^{(n)} = -(\partial_\xi P_1^{(n-1)})/(\omega_1 + \omega_2)$ with $P_1^{(0)} = \omega_2/(\omega_1 + \omega_2)l$. Inserting this solution in Eq. (44), we obtain a force-velocity relation $f_{\text{ext}} = f(v)$, with

$$f(v) = F_\Omega^{(0)} + (\eta + F_\Omega^{(1)})v + \sum_{n=2}^{\infty} F_\Omega^{(n)}v^n \quad , \tag{47}$$

where

$$F_\Omega^{(n)} = -\int_0^l d\xi\, P_1^{(n)} \Delta W' \quad , \tag{48}$$

and the prime denotes a derivative with respect to ξ. Using the definition Eq. (27) for the transition rates, we find the spontaneous force

$$F_\Omega^{(0)} = -\int_0^l d\xi \frac{\Delta W'}{\Omega + e^{-\Delta W/k_B T}} \quad . \tag{49}$$

This force is zero for a system which is not chemically driven, i.e. $\Omega = 0$ or if the system is symmetric. Similarly,

$$F_\Omega^{(1)} = \int_0^l d\xi \frac{(\Delta W')^2 e^{-\Delta W/k_B T} - \Omega' \Delta W'}{l\omega_2(\Omega + 1 + e^{-\Delta W/k_B T})^3} \tag{50}$$

is an effective friction coefficient which results from chemical transitions. For a passive system, this friction must be positive, $F_{\Omega=0}^{(1)} > 0$, which is indeed the case. For $\Omega \neq 0$, however, $f^{(1)}$ can become negative if $\Omega' \Delta W'$ is positive. This criterion implies that the function $\Omega(\xi)$ has maxima and minima at the same positions as ΔW. For W_1 periodic and W_2 constant this suggests e.g. placing the maxima of Ω at the positions of minimal W_1 which is the idea of localized excitations.

The fact that $F_{\Omega}^{(1)}$ can become negative suggests the possibility of an instability in the system. This can be discussed most easily by first considering a symmetric system with symmetric potentials and transition rates. In this case, the system is invariant under $(v, f_{\text{ext}}) \to (-v, -f_{\text{ext}})$, indicating that all even coefficients $f_{\Omega}^{(2n)} = 0$ vanish by symmetry. In this case,

$$f(v) = (\eta + F_{\Omega}^{(1)})v + F_{\Omega}^{(3)} v^3 + O(v^5) \quad . \tag{51}$$

If $F_{\Omega}^{(1)}$ is negative and decreases with increasing amplitude of Ω, an instability occurs as soon as $\Omega = \Omega_c$ for which

$$F_{\Omega_c}^{(1)} = -\eta \quad . \tag{52}$$

For $\Omega > \Omega_c$, the function $f(v)$ has a maximum, a minimum and a velocity interval where the effective friction

$$\eta_{\text{eff}} = \frac{\partial f(v)}{\partial v} \tag{53}$$

becomes negative, see Fig. 8. If no external force is applied, the system does not move for $\Omega < \Omega_c$ but two moving solutions bifurcate for $\Omega > \Omega_c$ with opposite velocity while the non-moving solution becomes unstable as revealed by a linear stability analysis. The system therefore at $\Omega = \Omega_c$ undergoes a bifurcation with spontaneous symmetry breaking which allows for the existence of spontaneous motion in the symmetric case.

If an external force is applied, the system can work against this force until the instability is reached at the minimum of the force velocity relation. Further increase of the force leads to a discontinuous change of the velocity. The system therefore shows the signature of a first-order transition with hysteretic behavior and for $f_{\text{ext}} = 0$ bistability where the selection of one of the stable states depends on the history of the system.

These arguments can be extended to the general case of a system with polar symmetry. In this case, all coefficients and in particular the spontaneous force $F_{\Omega}^{(0)}$ are nonzero. Dynamical transitions and instabilities do still exist but now occur typically for nonzero velocity and in an asymmetric way. A transition occurs if for increasing Ω a point with $\eta_{\text{eff}} = 0$ exists for a critical velocity v_c and for a critical force f_c. For $\Omega > \Omega_c$, a finite region with $\eta_{\text{eff}} = 0$ emerges and the function $f(v)$ has a maximum and a minimum. In this case, discontinuous changes of the velocity occur as a function of
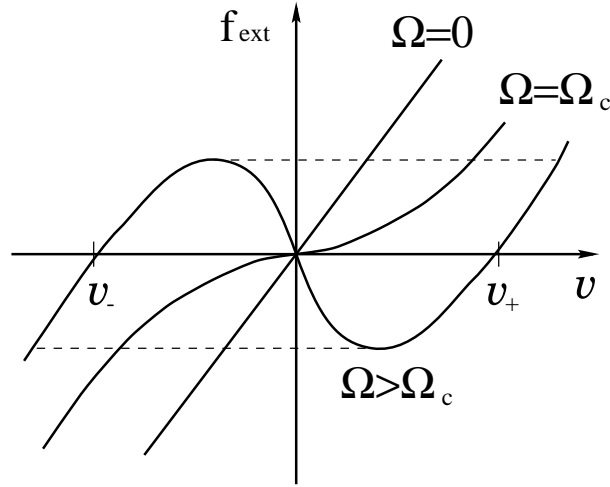
Fig. 8. Relation between velocity v and externally applied force f_{ext} for a symmetric system. For $\Omega < \Omega_c$ the system is passive. A dynamic transition with spontaneous symmetry-breaking occurs for $\Omega = \Omega_c$. For $\Omega > \Omega_c$, the system is actively moving with velocity $v_{\pm}$. The hysteresis is indicated by a broken line.

applied force as soon as the force reaches the extremal values where the system becomes unstable and the transition shows a hysteresis. A behavior with the characteristic as predicted by this theoretical analysis has been observed in motility assay experiments where electric fields are used to exert an external force [45].

4.3 Spontaneous oscillations

Another important consequence of the collectivity is the possibility to generate oscillatory motion if the system is acting together with elastic elements, see Fig. 7 (c). This corresponds to adding an elastic element to the force balance Eq. (44), which leads to

$$v = \frac{1}{\eta} \left[\int_0^l d\xi \, P_1 \Delta W' + f_{ext} - kx \right] \quad , \tag{54}$$

where $K = kN$ is the modulus of an external elastic element, k, the modulus per motor and

$$x(t) = \int_0^t dt' v(t') \quad , \tag{55}$$

is the total displacement of the system. First, we assume that the modulus k is small. In this case, the force varies slowly and we can use an adiabatic

approximation assuming that at any given time the system is in one of the steady states with

$$f_{\text{ext}} - kx = f(v) \quad , \tag{56}$$

where $f(v)$ is the force-velocity relationship introduced in Eq. (47). The change in velocity can be expressed as

$$\dot{v} = -\frac{Kv}{\eta_{\text{eff}}(v)} \quad . \tag{57}$$

This equation demonstrates that we expect an oscillatory instability to occur in this adiabatic limit, exactly if

$$\eta + F_\Omega^{(1)} < 0 \quad . \tag{58}$$

In this case, the non-moving state with $v = 0$ is unstable. As soon as the system starts moving an elastic force is created which opposes motion and leads to a decrease in velocity according to Eq. (57). As soon as an instability is reached with $\eta_{\text{eff}} = 0$, the velocity changes discontinuously in the opposite direction and the process is repeated. This scenario leads to characteristic relaxation oscillations of the position with a sawtooth like shape. For a symmetric system, the forward and backward parts of this process are identical and oscillations are symmetric with respect to $t \to -t$. In the asymmetric case, however, the asymmetry of the system is reflected in the shape of the oscillations, see inset of Fig. 9.

This adiabatic approximation is valid as long as the characteristic time η_{eff}/k is much longer than the transition times, i.e. $\eta_{\text{eff}}/k \gg \omega_1^{-1} + \omega_2^{-1}$. For large k and in particular close to the discontinuous transition with $\eta_{\text{eff}} = 0$, the full dynamic equations have to be taken into account. The onset of oscillatory motion can be determined by a linear stability analysis of the non-moving state with $v = 0$, and $x = x_0 = -f_\Omega^{(0)}/k$. For a small deviation from this initial state we write the ansatz

$$P_1(\xi, t) = R(\xi) + p(\xi)e^{st} \tag{59}$$

$$v(t) = ue^{st} \quad , \tag{60}$$

where $R \equiv P_1^{(0)}$ and $s = i\omega + \tau$ is complex. Here, ω is an oscillation frequency and τ a relaxation time. Inserting these expressions in Eq. (43), we find to linear order

$$p(\xi) = -u\frac{R'}{\alpha + s} \quad , \tag{61}$$

where we have defined $\alpha(x) = \omega_1(x) + \omega_2(x)$. Possible values of s are solutions to

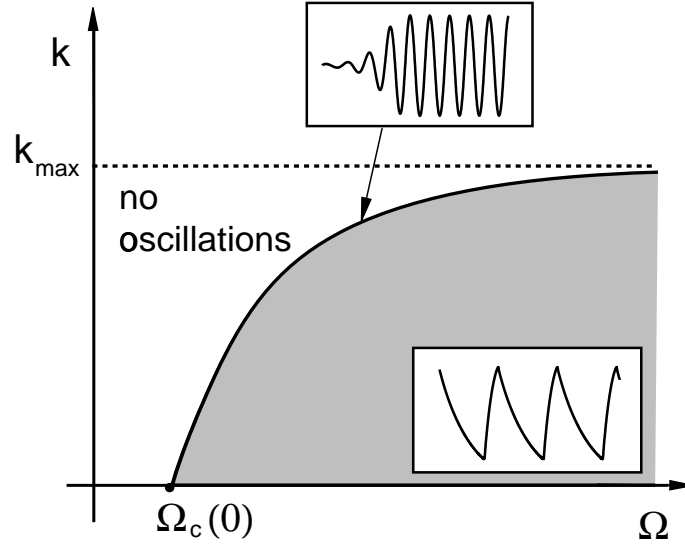$$\eta + \frac{k}{s} = -\int_0^l d\xi \, \frac{R' \Delta W'}{\alpha + s} \quad , \tag{62}$$

Fig. 9. Phase diagram for spontaneous oscillations as a function of the excitation activity Ω and the modulus per motor k of an external elastic element. The resting state becomes unstable with respect to oscillations along a line with $\Omega = \Omega_c(k)$. The insets show typical examples for oscillatory motion (displacement versus time): onset of sinusoidal motion at the instability and nonlinear oscillations with cusp-like shape for small k and large Ω.

As long as $\tau < 0$, the initial state is locally stable, it becomes unstable for $\tau = 0$ towards oscillatory motion with frequency ω. This instability is determined by setting $s = i\omega_c$. The frequency Ω_c at the instability obeys

$$\eta = -\int_0^l d\xi \frac{\alpha}{\alpha^2 + \omega_c^2} R' \Delta W' \tag{63}$$

$$k = \int_0^l d\xi \frac{\omega_c^2}{\alpha^2 + \omega_c^2} R' \Delta W' \quad . \tag{64}$$

For $k = 0$, we recover the criterion (58) with $\omega_c = 0$. The frequency at the instability increases as $\omega_c \sim k^{1/2}$ for increasing values of k. However, for $k > k_{\max}$ with

$$k_{max} = -\int_0^l R \Delta W'' \quad , \tag{65}$$

no instability occurs for arbitrarily large Ω see Fig. 9. Note, that $k_{\max}$ is given by the average negative curvature of the potential ΔW and can be roughly estimated by $k_{\max} \simeq U/l^2$, where U is the potential period. Note, that since k a modulus per motor, a motor collection of N motors can therefore undergo

oscillatory motion if working against an elastic element with rigidity smaller than $K < k_{\max} N$.

The nonlinear relation between force and velocity of steady states can be generalized to time-dependent external forces. Assuming that a limit cycle exists which is characterized by the Fourier representations

$$f_{\text{ext}}(t) = \sum_{n=-\infty}^{\infty} f_n e^{i\omega t}$$

$$v(t) = \sum_{n=-\infty}^{\infty} v_n e^{i\omega t}$$

$$(66)$$

a generalization of the expansion (47) is given by

$$f_n = F_n^{(0)} + F_{n,l}^{(1)} v_k + F_{n,lm}^{(2)} v_l v_m + F_{n,lmo}^{(3)} v_l v_m v_o + O(v^4) \quad . \quad (67)$$

The spontaneous force $F_n^{(0)} = F^{(0)} \delta_{n0}$ is nonvanishing only for the time independent mode $n = 0$. The linear response coefficient

$$F_{n,l}^{(1)} = \delta_{nl} \left[\eta + \frac{k}{i\omega l} + \int_0^l d\xi \frac{R' \Delta W'}{\alpha + i\omega l} \right] \quad (68)$$

vanishes at the instability. The real and the imaginary part of $F_{n,m}^{(1)}$ corresponds to an effective friction η_{eff} and to an effective elastic modulus $k_{\text{eff}}/i\omega$, respectively. Because of the non equilibrium nature of the systems both of these effective linear response coefficients can become negative which is impossible in an equilibrium situation.

Higher order coefficients can be obtained in a systematic way [29]. The expansion (67) characterizes the history-dependent response of the system to an external force which is periodic in time for small velocity amplitudes. As a result of time translation symmetry, the coefficients obey $F_{m,l_1..l_n}^{(n)} \sim \delta_{m,l_1+..+l_n}$. Spontaneous oscillations are solutions to Eq. (67) with $f_n = 0$ for all n which are well described near the instability. Far away from the instability nonlinearities become dominant. In the regime of small k, they are well captured by the adiabatic approximation given by Eq. (57).

5   Discussion and outlook

In the previous sections, we have described a generic framework to model the force and motion generation of molecular motors. The coupling of a chemical reaction to internal conformations and spatial degrees of freedom of a motor enzyme is described by an overdamped stochastic dynamics. Reducing the description to a simple two state model has the advantage to be sufficiently

simple for a theoretical analysis but still flexible to allow for a description of conditions of operation similar to those of motor molecules such as myosin or kinesin.

A quantitative modelization of motor enzymes on the molecular level is difficult. One the one hand experimental data is limited, on the other hand simplified models are not designed to describe all details of the functioning of complex enzymes. The properties of the two-state model discussed here depend of the choice of the potential shapes and on the conformation-dependence of the transition rates described by the functions $\alpha(x)$ and $\beta(x)$. These functions cannot be deduced from the molecular structure and are difficult to obtain experimentally. This is a general problem which is often referred to as unknown strain-dependence of transitions [34, 12]. The known force-velocity relation for single kinesin molecules is close to linear [51, 23]. Different models which have beed used to describe kinesin motion, all produce almost linear force-velocity relations and describe well the observed orders of magnitude [42, 40, 12, 10] which demonstrates that the basic properties of force-generation do not depend much on the choices made. It is however with the existing experimental data difficult to determine microscopic details of the force-generation process from a comparison with theory. We therefore refrain from a full quantitative comparison and focus our discussion on physical principles.

In biological situations, molecular motors are involved in processes such as muscle contraction, cell division and flagellar beating which are complex and involve large numbers of motors together with other enzymes which control and regulate the function of these systems. A physical approach to more complex situations is to avoid the complexity of control systems and to investigate the types of behavior which can result from the activity of many motors alone. The properties of larger-scale active systems can be studied using concepts of condensed matter physics. An important advantage of two-state models in this context is the possibility to start from a simple model for individual motors and to address the properties of many-motor systems. From such an approach the possibility of instabilities, dynamic transitions and spontaneous oscillations follows quite naturally. We therefore predict such behaviors to occur in biological situations. Related collective phenomena have recently been shown to exist also in other models [52, 43] which shows that the existence of dynamic instabilities in this class of systems is quite general.

The detailed conditions for which dynamic transitions will occur in biological systems such as coupled myosins or kinesins should depend on various parameters such as salt concentrations, temperature, motor density etc. Our approach does therefore not allow us to predict for which situations these new behaviors can in fact be found but provides a classification of the possible self-organized behaviors of such systems.

In vitro motility assays which use purified motors and filaments in an artificial environment are ideal systems to test these ideas and to study motor action in the absence of further biochemical regulatory systems. Motors grafted to a substrate set fluorescently marked filaments in motion which can easily be observed by standard light microscopy. The force-velocity relationship of the actin-myosin system has recently been determined by constraining filament motion along one direction by using linear grooves of $1\mu m$ in diameter as a substrate [45, 38], see Fig. 3 (d). Electric fields E applied parallel to the aligned and negatively charged actin filaments induce external forces which are homogeneously distributed along the filaments. The electrophoretic mobility $\mu = v/E$, where v is the velocity induced by an electric field E, measured for free filaments can be used to obtain an estimate for the external force per unit length $f \simeq 2\pi\mu\eta_w / \ln(r/d)E$ acting effectively on the filament. Here, eta_w is the viscosity of the solution and r and d are the radius of the filament and the distance between filament axis and the substrate. With this argument, we find that a field of $E \simeq 10^2 V/m$ induces a force per length of $f \simeq 1 pN/\mu m$ which is the order of magnitude of stall forces of an actin-myosin system [45].

In addition to providing the first force-velocity relations for a purified actin-myosin system, these experiments have revealed unexpected behavior for high myosin densities close to stall conditions. With increasing force applied against the direction of motion, filaments slow down, however before stalling completely an abrupt change in velocity to reverse motion has been observed. Since a histogram of the velocity distribution reveals two distinct maxima for different coexisting velocities and discontinuous changes of the velocity occur with a hysteretic behavior, a natural interpretation of this observation is a dynamic first order transition of the type predicted by our model. However, experiments of this type are difficult and measured values have significant uncertainties; more data is necessary to clearly prove the existence of the transition. Interestingly, macroscopic measurements of the behavior of muscles show near stalling conditions an unexpected rapid drop in velocity and a contracting state which is difficult to stabilize experimentally by feedback systems. This behavior could result from the averaged mechanical properties of many different filaments which individually show a transition of the type observed in motility assays. However, since complete muscles are very complex, other phenomena could be responsible.

In recent years, an increasing number of situation have been observed for which the concepts of dynamic instabilities in many-motor systems could be relevant. It is well known that the flight muscles of many insects generate oscillations themselves. These so-called asynchronous muscles show oscillatory behavior which is not triggered by a periodic nerve-signal [41]. These systems however are complete muscles for which the role of biochemical control systems could be important. Recently, it has become possible to study the active mechanical properties of single myofibrils, i.e. contractile fibers within

muscle cells, by using microneedles. Ordinary muscle myofibrils which under normal conditions simply contract, show spontaneous oscillations if put in specific conditions such as increased ADP concentration. Both tension- and length- oscillations were observed [54]. It was demonstrated that such oscillations continue to exist if regulatory enzymes bound to the actin-myosin motors were removed. These observations demonstrate that many muscles have such an instability in some region of parameter space [16]. Furthermore, this phenomenon seems to be a property of the actin-myosin system together with elastic elements. This observation is thus in the framework of our models consistent with the fact that the motility where the elastic elements are absent a first-order transition is observed.

Another important class of oscillating many-motor systems are cilia and flagella. These are hair-like appendages of many cells which are used for self-propulsion and to stir the surrounding fluid. They share the characteristic architecture of their core structure, the axoneme, a common structural motive that was developed early in evolution. It is characterized by nine parallel pairs of microtubules which are arranged in a circular fashion together with a large number of dynein molecular motors. In the presence of ATP, the dyneins attached to the microtubules generate relative forces while acting on neighboring microtubules. The resulting internal stresses induce the bending and wave-like motion of the axoneme [2].

These systems are very complex, show various patterns of motion and regulatory systemscould play an important role. A model in two-dimensions for an internally driven filament can be used to demonstrate that a dynamic instability of the many-motor system most naturally generates oscillating motion and wave-like propagating shapes which can be used for self-propulsion [9]. This idea that simple patterns of motion are induced via a dynamic instability is supported by the observations that flagellar dyneins are able to generate oscillatory motion on microtubules [47], and that isolated and de-membranated flagella in solution containing ATP above a threshold concentration swim with a simple wave-like motion [17]. It suggest, that basic wave-like patterns of motion are generated by a self-organized motor-induced mechanism and that sophisticated regulatory systems may have evolved at a later time to fine tune the system and to generate new patterns of motion.

References

1. Ajdari A., and Prost J. (1992): C.R. Acad. Sci. Paris II, **315**, 1635.
2. Alberts B., Bray D., Lewis J., Raff M., Roberts K. and Watson J.D. (1994): The molecular biology of the cell, (Garland, New York).
3. Astumian R.D., and Bier M. (1994): Phys. Rev. Lett. **72**, 1766.
4. Astumian R.D. (1997): Science **276**, 917.

5. Block S.M. (1998): J. Cell. Biol. **140**, 1281.

6. Büttiker, M. (1987): Z. Phys. B **68**, 161.

7. Chauwin J.F., Ajdari A., and Prost J. (1994): Europhys. Lett. **27**, 421.

8. Chauwin J.F., Ajdari, and Prost J. (1995): Europhys. Lett. **32**, 373.

9. Camalet S., Jülicher F., and Prost J. (1998): preprint cond-mat/9810279.

10. Derényi I., and Vicsek T. (1996): Proc. Nat. Acad. Sci. **93**, 6775.

11. Doering C.R. (1995): Nuovo Cimento **17**, 685.

12. Duke T., and Leibler S. (1996): Biophys. J. **71**, 1235.

13. Faucheux L.P., and Libchaber A. (1995): J. Chem. Soc. Farad. Trans. **91**, 3163.

14. Feynman R.P., Leighton R.B., and Sands M. (1966): *The Feynman Lectures on Physics* (Addison-Wesley, Reading MA), Vol. I, Chap. 46.

15. Finer J.T., Simmons R.M., and Spudich J.A. (1994): Nature **368**, 113.

16. Fujita H. and Ishiwata S. (1998): Biophys. J. **75**, 1439.

17. Gibbons I.R. (1975): in *Molecules and Cell Movement*, S. Inoué and R.E. Stephens (Eds.), Raven Press, New York.

18. Gilbert S.P., Webb M.R., Brune M., and Johnson K.A. (1995): Nature **373** 671.

19. Gorre L., Ioannidis E., and Silberzan P. (1996): Europhys. Lett. **33**, 267.

20. Gorre-Talini L., Spatz J.P., and Silberzan P. (1998): Chaos **8** 650.

21. Harada Y., Noguchi A., Kishino A., and Yanagida T. (1987): Nature **326**, 805.

22. Hill T.L. (1974): Prog. Biophys. Mol. Biol. **28**, 267.

23. Hunt A.J., Gittes F., and Howard J. (1994): Biophys. J. **67**, 766.

24. Huxley A.F. (1957): Prog. Biophys. **7**, 255.

25. Huxley A.F., and Simmons R.M. (1971): Nature **233**, 533.

26. Huxley H.E. (1969): Science **164**, 1365.

27. Ishijima A., Doi T., Sakurada K., and Yanagida T. (1991): Nature **352** 301.

28. Jülicher F., and Prost J. (1995): Phys. Rev. Lett. **75**, 2618.

29. Jülicher F., and Prost J. (1997): Phys. Rev. Lett. **78**, 4510.

30. Jülicher F., Ajdari, A. and Prost J. (1997): Rev. Mod. Phys. **69** 1269.

31. Kreis T., and Vale R. (1993): *Cytoskeletal and Motor Proteins*, (Oxford University Press, New York).

32. Kron S.J. and Spudich J.A. (1986): Proc. Natl. Acad. Sci. USA **83**, 6272.

33. Landauer R. (1988): J. Stat. Phys. **53**, 233.

34. Leibler, S., and Huse D. (1993): J. Cell Biol. **121**, 1357.

35. Lymn R.W., and Taylor E.W. (1971): Biochem. **10**, 4617.

36. Magnasco M.O. (1993): Phys. Rev. Lett. **71** 1477 (1993).

37. Nédélec F.J, Surrey T., Maggs A.C. and Leibler S. (1997): Nature **389**, 305.

38. Ott A, contribution in this volume.

39. Peskin C.S., Ermentrout G.B., and Oster G.F. (1994): *Cell Mechanics and Cellular Engineering*, V.Mow et al eds. (Springer, New-York).

40. Peskin C.S., and Oster G.F. (1995): Biophys. J. **68**, 202.

41. Pringle J.W.S. (1977): in *Insect Flight Muscle*, R.T. Tregear, Ed. , North-Holland, Amsterdam, 177.

42. Prost J., Chauwin J.F., Peliti L., and Ajdari A. (1994): Phys. Rev. Lett. **72**, 2652.

43. Reimann P., Kawai R., Van den Broek C., and Hänggi P. (1998): preprint.

44. Risken H. (1984): *The Fokker-Planck Equation* (Springer, Berlin).

45. Riveline D., Ott A., Jülicher F., Winkelmann D.A., Cardoso O., Lacapère J.-J., Magnusdottir S., Viovy J.-L., Gorre-Talini L. and Prost J. (1998): Eur. Biophys. J. **27** 403.
46. Rousselet J., Salome L., Ajdari A., and Prost J., 1994, Nature **370**, 446.
47. Shingyoji C., Higuchi H., Yoshimura M., Katayama E., and Yanagida T. (1998): Nature (London) **393**, 711.
48. Spudich J.A. (1990):, Nature **348**, 284.
49. Schnitzer M. and Block S.M. (1997): Nature **388** 386.
50. Svoboda K., Schmidt C.F., Schnapp B.J., and Block S.M. (1993): Nature **365**, 721.
51. Svoboda K, and Block S. (1994): Cell **77**, 773 (1998).
52. Van den Broeck C., Reimann P., Kawai R., and Hänggi P. (1998): preprint.
53. Winkelmann D.A., Bourdieu L., Ott A., Kinose F., and Libchaber A. (1995): Biophys. J. **68** 2444.
54. Yasuda K., Shindo Y. and Ishiwata S. (1996): Biophys. J. **70**, 1823.